

Dispersion analysis of the unignited flare gas in an LNG-FPSO vessel

Chongmin Kim¹ · Byung Chul Choi[†]

(Received April 14, 2017 ; Revised June 22, 2017 ; Accepted August 22, 2017)

Abstract: A liquid natural gas floating production, storage, and offloading (LNG-FPSO) unit is a floating vessel used as an offshore plant in order to liquefy and store natural gas until it is offloaded onto an LNG carrier. LNG-FPSOs are incorporated with the new concept of LNG value chain formation, which can be more economical than conventional methods for the development of small- or medium-scale gas fields. A typical approach is implemented for large-scale gas fields by establishing a direct connection between an existing offshore platform and an onshore LNG plant using a pipeline. However, because the facilities required for all processes are designed within a confined space on the vessel, the structure of this vessel may be fundamentally charged with a higher risk of fire or explosion due to the dispersion of flammable gas, which results from accidental leaks of LNG. For the safety design, therefore, quantitative evaluation of the LNG-FPSO is required for understanding the major potential hazards imposed on the personnel, assets, and environment. In this study, a numerical analysis on the dispersion characteristics of the unignited flare gas ejected from a vent mast was performed as a part of quantitative risk assessment (QRA) in the front-end engineering and design (FEED) stage. The results for the selected scenarios showed that the extents of flammable limits evaluated by the concentration distributions of flammable gas released from the vent mast could be acceptable for the helideck, including accommodation as well as all topsides on the basis of CAP 437 Safety Regulation. In the next stage for EPC, a detailed analysis reflecting the variation of environmental conditions will be further required to determine the design specification of flare towers.

Keywords: LNG-FPSO, Gas dispersion, Unignited flare gas, Flammable limits, Computational Fluid Dynamics (CFD)

1. Introduction

The technology to acquire energy resources from the subsea using offshore plants is attracting increasing interest because of the depletion of energy resources on land. The International Maritime Organization (IMO)'s "Global Sulfur Cap 2020" should issue caution related to works in the maritime area [1]. Therefore, the demand for liquefied natural gas (LNG) as a clean fuel is expected to increase with the need for developing the natural gas field in the subsea. The application of the pipeline had major economic problems during the development of deep-sea gas fields. It is a high-cost network that links pipelines from offshore gas fields to land-based liquefaction and storage plants. In order to meet these demands, LNG-floating production, storage, and offloading (FPSO) have been introduced in an offshore plant. The LNG-FPSO ship was clearly designed for the function of liquefying the gas mined from the submarine gas field after pre-treatment, and storing the liquefied gas until it was unloaded to the LNG carrier. An FPSO

has the advantage of reuse capability by moving to another gas field [2]. The operations of LNG-FPSOs on offshore installations and onshore LNG plants are performed on a single limited-scale vessel. Therefore, the performance that reflects safety designs and reliability analysis through quantitative risk assessment (QRA) was considered one of the most important issues [3]. Accidental leaks or releases during the process of LNG-FPSO results in the dispersion of flammable or liquid-induced evaporative gases. There may be certain scenarios in which the consequences of a fire or explosion may be greatly enhanced by the ignition sources within the flammable limits [4][5]. In this regard, understanding the dispersion characteristics of LNG leakage is an essential issue for safety design against fire and explosion damage to life and property.

This section reviews recent studies on the fundamental dispersion of LNG release. The wind tunnel experiments were conducted using isothermal heavy gas and cryogenic gas, respectively. The numerical model was simulated using LNG

[†] Corresponding Author (ORCID: <http://orcid.org/0000-0002-7427-6697>): R&D Center, KR, 36, Myeongji ocean city 9-ro, Gangseo-gu, Busan, 46762, Republic of Korea, E-mail: byungchul.choi@hotmail.com, Tel: 070-8799-8591

¹ R&D Center, Korean Register of Shipping, E-mail: ckim@krs.co.kr, Tel: 070-8799-8746

This is an Open Access article distributed under the terms of the Creative Commons Attribution Non-Commercial License (<http://creativecommons.org/licenses/by-nc/3.0>), which permits unrestricted non-commercial use, distribution, and reproduction in any medium, provided the original work is properly cited.

gas by applying gas diffusion around the obstacle, which was then successfully compared with the experiments of the concentration profiles [6]. Two-dimensional (2D) computational fluid dynamics (CFD) simulations of the transient spatial concentration fields were conducted to investigate the features of the flammable regions, due to the release of boil-off gas into the atmospheric air through a vertical pipe [7]. Moreover, LNG dispersion analysis was performed using CFD with respect to various environmental conditions, and the effects of release over two scenarios on water and concrete were analyzed and compared with those of previous experiments [8].

As a study on engineering solutions to practical problems, numerical simulations were performed on gas cloud dispersion using actual data from a sea-trial test for boiling off gas released from the vent mast of an LNG carrier. The evaluation based on the IMO IGC code emphasized the importance of reevaluation of the vent mast exit height [9]. However, the practical application of the gas dispersion analysis for marine floating LNG plants, such as LNG-FPSOs, in the LNG value chain was disclosed to the public only to a limited extent.

In this study, the gas dispersion simulations have been performed to evaluate the flammable limits of gas released from the vent mast on the topside area of LNG-FPSO. The main objectives of this study are to simulate the flammable gas concentration on a specified location by identifying any gas dispersion scenarios limited by unignited flare gas at the flare tower height, and highlight the areas in which the flammable limit criteria are exceeded, as well as to recommend the safety action for protection of personnel and equipment, if required.

2. General Description

The LNG-FPSO is a floating unit equipped with a natural gas liquefaction plant on its topside. The installation was to be located offshore approximately 60 km from the coastline, in a water depth of approximately 2,000 meters. The installation has facilities to receive, pre-treat, and liquefy the incoming gas, and to store and offload the products (LNG, liquid propane, liquid butane, and condensate). In summary, the installation has the following main characteristics:

Table 1: Principal dimensions for the LNG production system

Overall Length	~ 420.0 m
Length Between Perpendiculars	420.0 m
Breadth	70.0 m
Depth	35.0 m
Max. Operating Draft	16.0 m
Hull Scantling Draft	16.5 m
Flare Height	215.0 m

- Gas plant (receive, pre-treat and liquefy), comprising safety-related facilities and receiving system (turret and pull-in facilities),
- Storage and offloading of LNG,
- Storage and offloading of LPG,
- Storage and offloading of C5+,
- Utilities necessary to keep the installation's stand-alone operation,
- Safety systems to ensure the safety of the installation for the intended purpose.
- Power generation system to meet all the needs of the installation,
- Accommodation block/Living quarters,
- Ventilation and air conditioning system for the accommodation block and other mechanical ventilated/conditioned rooms,
- Cargo handling systems, including cranes, monorails, rail cars, and related facilities,
- Helideck, suitable for Sikorsky S-61, S-92, and ASS332L2-Super puma helicopter landing, and
- Telecommunication facilities.

The hull design includes a turret, the marine and ship system, cargo system, offloading, mooring, living quarters, helideck and power generation. In addition, the topside design and layout includes gas treatment and gas fractionation with LNG liquefaction installed on topsides modules. As per the installation, the principal dimensions are summarized in **Table 1**.

3. Methodology

3.1 Computational Method

The following steps were followed to perform the gas dispersion analysis, executed through Kameleon FireEX (KFX). The first step involves the conversion of the model file for KFX simulation. To define the structural system, involving geometry information and boundary conditions, the DGN-file structure as a three-dimensional (3D) computer-aided design (CAD) model was translated to the KFX file format by using the KFX software. The vent mast dispersion scenarios involve various parameters related to release location, direction, and flow rate, along with wind speed and direction. In order to conduct a KFX simulation, an appropriate KFX model file was manipulated with the dataset of the selected scenario. The specific control parameters were appropriately chosen by considering the simulation time and reliability of analysis. The probabilistic analysis was not incorporated in this work. In general, the probabilistic calculations in the total risk assessment may consider thousands of scenarios, combining different release

rates, release locations, wind conditions, release volumes, etc., while only very limited number of scenarios can be operated with CFD-codes. Thus, the results from the simulations should not be used directly during design, but as support for QRA in the front-end engineering and design (FEED) package.

The system of equations is solved by applying a low-pass filter using the large-eddy simulation technique, in which the small-scale eddies that pass through the grid are modeled, and the large-scale eddies are computed, respectively. The low-pass filter width is taken as the cube root of cell volume. KFX is based on the finite difference method, which implements a predictor-corrector scheme explicitly with second-order accuracy in space and time. It is not suitable for complex-shaped geometries, as it uses rectilinear meshing, but it helps in faster computation. More details on the physical concepts are given in the KFX user & theory manuals [10][11].

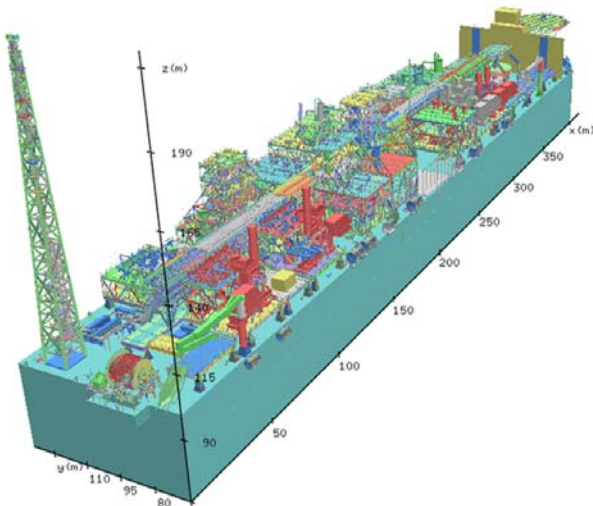


Figure 1: 3D KFX model of LNG-FPSO geometry

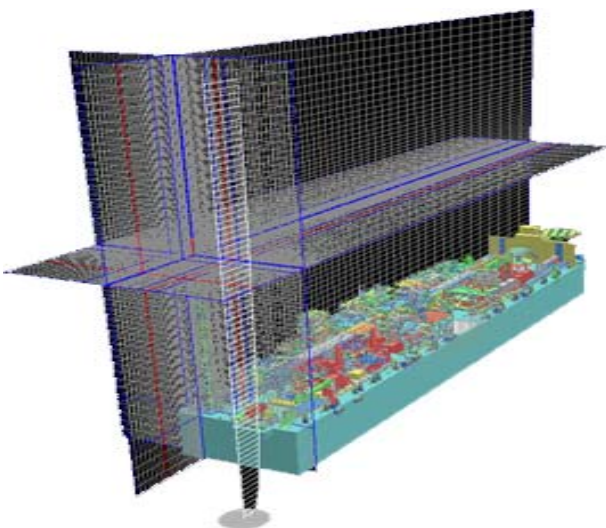


Figure 2: 3D grid system of the geometry

3.2 3D CAD Model and Grid Generation

According to the conversion procedure of the DGN file to a KFX file for the topside and hull structure, the files have been translated to KFX geometry format using the KFX tool. An overview of the KFX model is shown in **Figure 1**. For the KFX geometry, the calculation domain for the dispersion simulation of unignited flare gas was $480 \text{ m} \times 120 \text{ m} \times 285 \text{ m}$, and $\sim 5 \times 10^5$ cells were used, with the smallest control volume of $0.0423 \text{ m} \times 0.001 \text{ m} \times 0.001 \text{ m}$. The smallest grid cell was used with the cell size growing outwards in all directions from the release cell. Hence, the mesh geometry was well represented in **Figure 2**, while larger grid sizes, placed far away from the release cell, were coarser and had less accuracy. Because the minimum control volumes for each calculation were automatically determined from the expanded jet diameter for choked flow, they tended to generate grids with a very large aspect ratio for control volumes far away from the release point. However, the optimized grid resolution was chosen by the KFX built-in wizard to obtain a result of sufficiently accurate and efficient simulations [10][11].

3.3 Governing Equations

The governing equations were solved using partial differential equations (PDEs) to describe the transient behavior of different field variables in space. The PDEs describing fluid flow are commonly referred to as transport equations and are comprised of transient, convective, diffusion, and source equations. In this non-reacting gas-dispersion simulation, the source term and radiative heat flux were ignored. The equations representing mass, momentum, energy, and species are shown below with the ideal gas equation.

- Conservation of mass:

$$\frac{\partial \rho}{\partial t} + \nabla \cdot (\rho \mathbf{u}) = 0 \quad (1)$$

- Conservation of momentum:

$$\frac{\partial \rho \mathbf{u}}{\partial t} + \nabla \cdot (\rho \mathbf{u} \mathbf{u}) = -\nabla p + \nabla \cdot \boldsymbol{\tau} + \rho \mathbf{g} \quad (2)$$

- Conservation of energy:

$$\frac{\partial \rho h_s}{\partial t} + \nabla \cdot (\rho \mathbf{u} h_s) = \frac{Dp}{Dt} - \nabla \cdot \dot{\mathbf{q}}'' + \boldsymbol{\tau} \cdot \nabla \mathbf{u} \quad (3)$$

- Conservation of species:

$$\frac{\partial \rho Y_i}{\partial t} + \nabla \cdot (\rho \mathbf{u} Y_i) = -\nabla \cdot \mathbf{J}_i \quad (4)$$

- The Equation of state:

$$p = RT \sum_{i=1}^n \frac{Y_i}{w_i} \quad (5)$$

where ρ is the density, \mathbf{u} is the velocity vector, p is the pressure, $\boldsymbol{\tau}$ is the viscous stress tensor, \mathbf{g} is the gravitational acceleration, h_s is the sensible enthalpy, $\dot{\mathbf{q}}''$ is the heat flux, Y_i is the mass fraction of species i , \mathbf{J}_i is the diffusive flux, R is the universal gas constant, T is the temperature, and w_i is the molecular weight of species i .

4. Result & Discussion

4.1 Selected Release Scenarios

Based on the previous data of the flare radiation study [12], in this study, four release scenarios and the gas compositions for all the release scenarios were selected as below:

- Scenario 01: High Pressure (HP) Warm Flare,
- Scenario 02: High Pressure (HP) Cold Flare,
- Scenario 03: Low Pressure (LP) Warm Flare, and
- Scenario 04: Low Pressure (LP) Cold Flare.

The HP Warm flare was composed of hydrocarbon vapors, amines, water, and liquid hydrocarbons from various high-pressure sources in the process. The HP Cold flare was composed of hydrocarbon vapors and liquid hydrocarbons from various high-pressure sources in the liquefaction system. The LP Warm flare was composed of hydrocarbon vapors from various low-pressure sources in the process, and the LP Cold flare was composed of hydrocarbon vapors and liquid hydrocarbons from various low-pressure sources from the liquefaction, refrigerant, and boil-off gas (BOG) systems. These flares relieve the pressure resulting from the combination of any single safety system with any possible process failure.

The chemical compositions of each flare for different scenarios are given in **Table 2**. The pseudo-fuels are defined with respect to the scenarios in **Table 3**. A common location of the release points was then chosen with no obstruction in the initial development of the jet at the flare tower tip. Data for the reservoir, surroundings, and release rates were specified for the gas dispersion scenario as a calculation input. In addition, a release diameter was specified. Further, the equivalent release parameters, such as the initial release velocity and hole diameter, were estimated. The physical data applied for jet releases are listed in **Table 4**.

It is noted that, due to high pressure and corresponding small release diameter, the simulated releases in the process area resulted in a highly under-expanded jet with a shock structure, which would have required a compressible solver and extensive grid refinement to resolve. Thus, the KFX-tool “Jet boundary conditions calculator” was used to calculate the expanded jet conditions at the downstream of the original release point. Jet boundary conditions calculator is a tool in the KFX software that calculates inlet conditions for supersonic jet releases. The jet boundary condition method utilized ideal gas relations and conservation of mass, momentum, and energy to predict the downstream fluid state of the shock structure. Air entrainment into the highly turbulent jet was also taken into account using this method. When the high-pressure gas was discharged through an opening ejection point into an atmosphere, the released gas would expand very rapidly to the ambient pressure. The complex expansion process of high-pressure gas releases was modeled using the pseudo-source concept to reduce the computational costs for simulation cases of practical interest.

Table 2: Chemical compositions of flares

Gas composition			N2	CO2	C1	C2	C3	C4	C5	C6	C7	C8	C9	C10	H2O	
Volume percent [%]	HP	Warm	0.47	1.36	79.70	5.23	2.18	0.91	0.15	0.33	0.15	0.83	0.02	0.22	9.20	
		Cold	7.09	0	27.42	36.94	28.55	0	0	0	0	0	0	0	0	0
	LP	Warm	2.22	0	97.77	0.01	0	0	0	0	0	0	0	0	0	0
		Cold	5.62	0	94.37	0.01	0	0	0	0	0	0	0	0	0	0

Table 3: Pseudo-fuels

Gas condition	Value				Note
	HP		LP		
	Warm	Cold	Warm	Cold	
Composite fuel	C1.2H4.4		C2.01H6.02		Calculated
LFL [%]	4.4247		2.9596		Calculated
UFL [%]	14.3199		11.9292		Calculated
Stoichiometric [%]	8.3573		5.6348		Calculated
Molecular weight of hydrocarbon [kg/kmol]	18.8346		30.1703		Calculated
Molecular weight of mixture [kg/kmol]	19.1438		30.0164		Calculated

Table 4: Physical data applied for jet releases

Gas condition	Value				Note
	HP		LP		
	Warm	Cold	Warm	Cold	
Reservoir temperature [°C]	5	-59	15	-160	Ref. [12]
Reservoir pressure [barg]	4	4	0.2	0.2	Ref. [12]
Flow rate [kg/s]	177.67	319.81	11.84	33.33	Ref. [12]
Hole diameter [m]	0.485389	0.6084	0.2980	0.3933	Calculated
Location (X, Y, Z) [m]	8.6, 121.3, 215.5	8.6, 121.3, 215.5	8.6, 121.3, 215.5	8.6, 121.3, 215.5	
Direction	+Z	+Z	+Z	+Z	

In addition, KFX uses the log-law wall boundary to enable reasonable calculations of shear stress, heat flux, and mass flux from a fluid to a solid wall in a relatively coarse grid. More details about the physical background for the methods used are given in the KFX theory manual [11].

4.2 Ambient Condition

Table 5 exhibits the logarithmic wind boundary profile set with the ambient temperature and atmospheric pressure for domain calculation. Considering the two reference wind conditions, eight simulations were carried out in total.

Table 5: Ambient conditions

Wind condition	Value	Note
Wind direction [deg. from north]	270	West
Reference wind speed [m/s]	10/20	Ref. [12]
Wind profile ground level [m]	65	-
Ground roughness [m]	0.0002	
Atmospheric stability	N	Neutral class
Ambient temperature [°C]	33	-

4.3 Simulation Results

Long-term relief scenarios for any excess hydrocarbon gases from the process and utility systems during start-up, operational, and emergency conditions would be reasonable, in order to examine the dispersion distance of the ejected gas as a conservative investigation. Therefore, the simulations were calculated up to ~300 s in real time after saturation, i.e., until the fuel/carbon balance attained a steady state in the domain.

Important results depending on the purpose of each scenario and visualization of the gas concentration to demonstrate the flammable limits were presented and discussed in this chapter. The release point and release direction, as well as the wind direction, would be easily understood in the gas concentration plots. The pictures described in this paper are based on the

human perception to an extent, with a fair representation of the appearance of gas dispersions.

As a result, the mole percent of unignited flare gas discharged from the flare tip into the ambient air was presented using the stepped ranges, as shown in **Figure 3** for HP-warm, **Figure 4** for HP-cold, **Figure 5** for LP-warm, and **Figure 6** for LP-cold, as an account of eight selected scenarios with respect to the gas releases and wind conditions. The gas dispersion results were investigated to assess the flammable limits for the following locations:

- Helideck and helicopter approach and
- All topside modules.

In this study, the maximum extension of the unignited flare gas in the ambient air was estimated with respect to the lower flammable limit (LFL), which is less than the mole percent of ~5.0%, 50% LFL (less than the mole percent of ~2.5%), 10% LFL (less than the mole percent of ~0.5%), and below that, as shown in **Figure 3 ~ Figure 6**. The maximum permissible concentration of hydrocarbon gas was set to 10% LFL. The analysis was focused on the flammable gas concentration on the helideck in order to meet the requirement, as per the CAP 437 Safety Regulation [13].

Reference [13] stated that the maximum permissible concentration of hydrocarbon gas within the helicopter operating area is 10% LFL. Concentrations above 10% LFL have the potential to cause helicopter engines to surge and/or flame out with the consequent risk to the helicopter and its passengers. It should also be appreciated that, in forming a potential source of ignition for flammable gas, the helicopter can pose a risk of the installation itself.”

As listed in **Table 6**, the selected scenarios showed that the mole percent of gas in the ambient air were below the acceptance criterion of 10% LFL for the target area, which includes the helideck (located on the top of the accommodation) and topside modules.

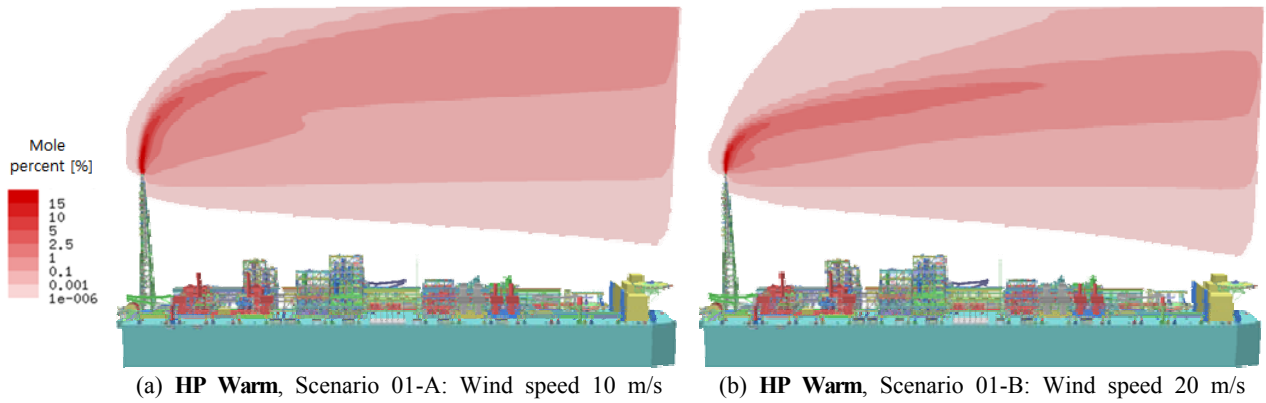


Figure 3: Flammable limits with the release rate of 177.67 kg/s

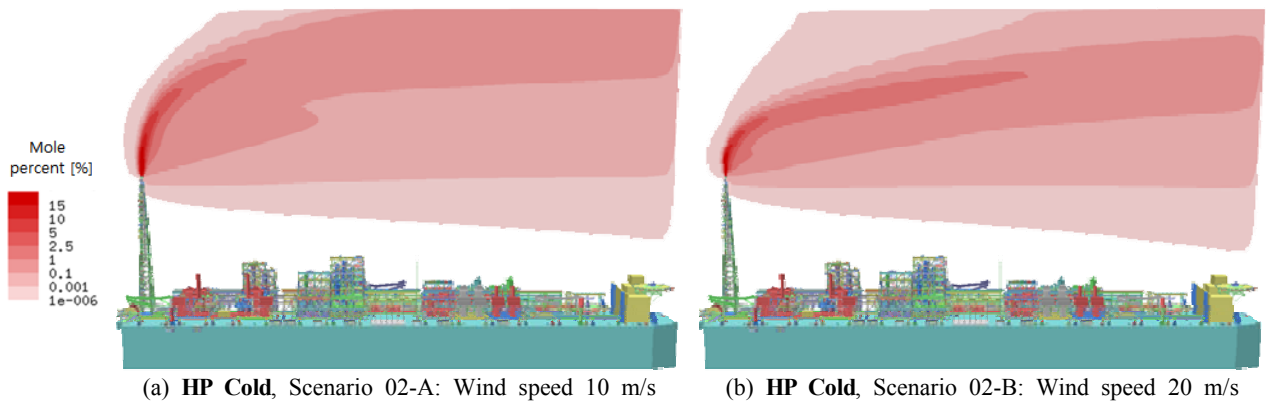


Figure 4: Flammable limits with the release rate of 319.81 kg/s

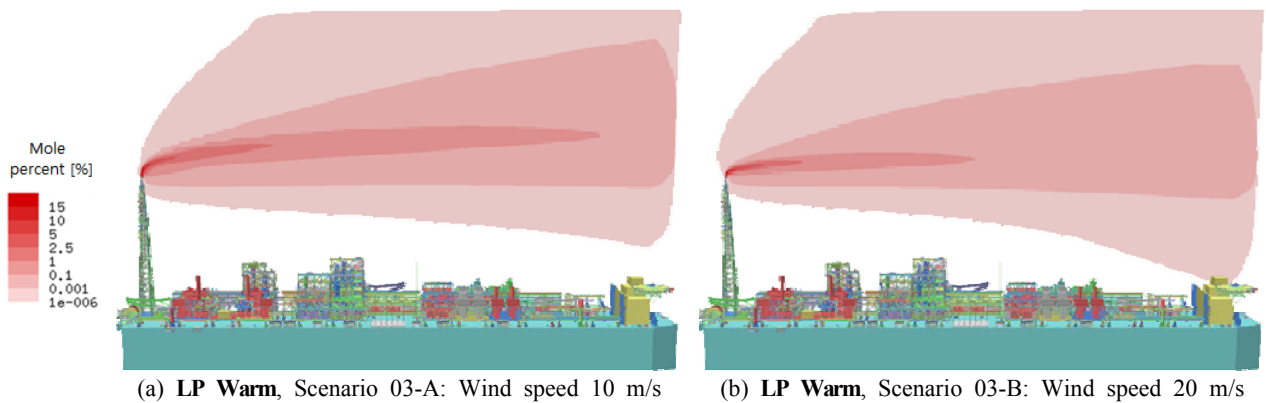


Figure 5: Flammable limits with the release rate of 11.84 kg/s

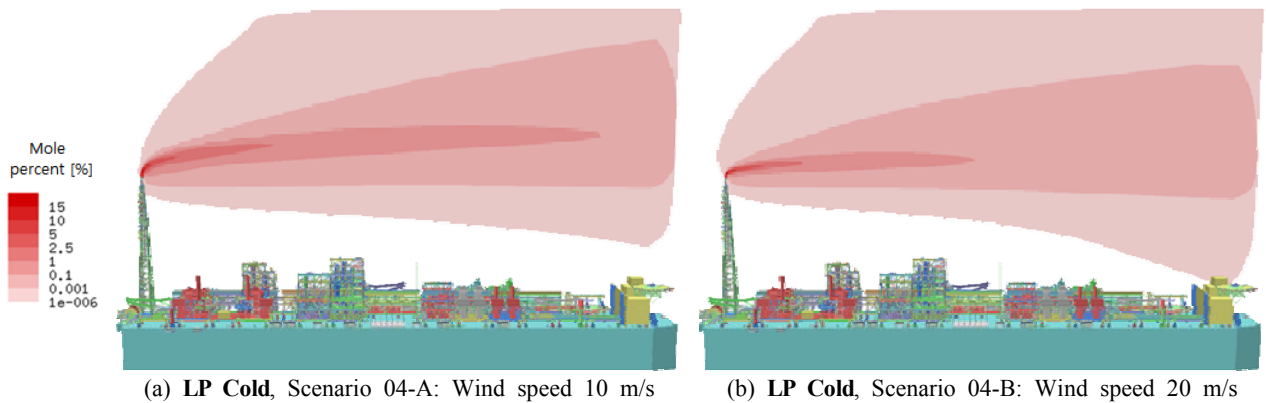


Figure 6: Flammable limits with the release rate of 33.84 kg/s

Table 6: Mole percent specific to target location [mol. %]

Wind speed/ Target location		HP		LP	
		Warm	Cold	Warm	Cold
10 m/s	Helideck	0	0	0	0
	Topside	0	0	0	0
20 m/s	Helideck	0	0	< 0.001	< 0.001
	Topside	0	0	0	0

5. Conclusion

For the purpose of the FEED package of LNG-FPSOs, CFD simulations of unignited flare gas dispersion analysis were conducted using KFX commercial software in order to confirm the LFL criteria in target areas, based on the CAP 437 Safety Regulation. The results demonstrated that the flammable gas concentration did not exceed the maximum permissible concentration of hydrocarbon gas on the helideck, as follows.

- LFL for HP Warm - acceptable (below 10% LFL)
- LFL for HP Cold - acceptable (below 10% LFL)
- LFL for LP Warm - acceptable (below 10% LFL)
- LFL for LP Cold - acceptable (below 10% LFL)

The effect of flammable gas concentration on all topside modules was negligible. The final dispersion analysis, reflecting the detailed conditions, will be performed by safety engineers after confirming the flare tower height in the engineering, procurement, and construction (EPC) phase for the LNG-FPSO project.

Acknowledgement

This research was supported by a grant from the LNG Plant R&D Center funded by the Ministry of Land, Infrastructure, and Transport of the Korean government.

Reference

- [1] The Secretariat of the IMO, IMO Official Web Site, [http://www.imo.org/en/OurWork/Environment/PollutionPrevention/AirPollution/Pages/Sulphur-oxides-\(SOx\)--Regulation-14.aspx](http://www.imo.org/en/OurWork/Environment/PollutionPrevention/AirPollution/Pages/Sulphur-oxides-(SOx)--Regulation-14.aspx), Accessed October 25, 2017.
- [2] J. K. Paik and A. K. Thayamballi, *Ship-shaped Offshore Installations: Design, Building and Operation*, Edition 1, London, UK: Cambridge University Press, 2007.
- [3] A. Brandsæter, "Risk assessment in the offshore industry," *Safety Science*, vol. 40, no. 1-4, pp. 231-269, 2002.
- [4] J. A. Suardin, A. J. McPhate Jr, A. Sipkema, M. Childs, and M. S. Mannana, "Fire and explosion assessment on oil and gas floating production storage offloading (FPSO) : An effective screening and comparison tool," *Process Safety and Environmental Protection*, vol. 87, no. 3, pp. 147-160, 2009.
- [5] S. Dana, C. J. Lee, J. Park, D. Shin. and E. S. Yoon, "Quantitative risk analysis of fire and explosion on the top-side LNG-liquefaction process of LNG-FPSO," *Process Safety and Environmental Protection*, vol. 92, no. 5, pp. 430-441, 2014.
- [6] R. Ohba, A. Kouchi, T. Hara, V. Vieillard, and D. Nedelka, "Validation of heavy and light gas dispersion models for the safety analysis of LNG tank," *Journal of Loss Prevention in the Process Industries*, vol. 17, no. 5, pp. 325-337, 2004.
- [7] S. Fardisi and G. A. Karim, "Analysis of the dispersion of a fixed mass of LNG boil off vapour from open to the atmosphere vertical containers," *Fuel*, vol. 90, no. 1, pp. 54-63, 2011.
- [8] B. R. Cormier, R. Qi, G. Yun, Y. Zhang, and M. Sam Mannan, "Application of computational fluid dynamics for LNG vapor dispersion modeling: A study of key parameters," *Journal of Loss Prevention in the Process Industries*, vol. 22, no. 2, pp. 332-352, 2009.
- [9] H. K. Kang, "An examination on the dispersion characteristics of boil-off gas in vent mast exit of membrane type LNG carriers," *Journal of the Korean Society of Marine Environment & Safety*, vol. 19, no. 2, pp. 225-231. 2012.
- [10] B. E. Vembe, R. N. Kleiveland, B. Grimsmo, N. I. Lilleheie, K. E. Rian, R. Olsen, B. Lakså, V. Nilsen, J. E. Vembe, and T. Evanger, "Kameleon FireEx KFX® Furcifer User Guide," Computational Industry Technologies AS (ComputIT), February 14, 2014.
- [11] B. E. Vembe, K. E. Rian, J. K. Holen, N. I. Lilleheie B. Grimsmo, and T. Myhrvold, "Kameleon FireEx 2000 Theory Manual," Computational Industry Technologies AS (ComputIT), June, 2001.
- [12] Hyundai Heavy Industries (HHI), "Flare Radiation Study Report," LFPT-HHI-P-00-DOC-008, July, 2015.
- [13] Civil Aviation Authority (CAA), "Offshore Helicopter Landing Areas: Guidance on Standards," Edition 8, UK, CAP 437, December, 2008.